Biorthogonal Wavelet Analysis on 2D EM Scattering from Large Objects

Qinke Zhang and Nathan Ida
Department of Electrical Engineering, The University of Akron, Akron, OH 44325-3904 USA

Abstract- **This paper investigates the potential advantages of wavelet analysis for large scale problems in EM scattering. A biorthogonal wavelet-based MoM is used in analyzing 2D EM scattering from a conducting structure. Numerical examples show that wavelet-based MoM is especially suitable for analysis of large problems in the sense that the sparseness of the resulting matrices becomes more apparent with increase of the electrical size of scatterers.**

Index terms- **Biorthogonal wavelets, moment method, electromagnetic scattering, sparse matrix.**

I. INTRODUCTION

Wavelets have proven to be of many advantages over other standard methods in signal and image processing. In numerical analysis wavelets also offer important features. One is that the resulting matrix is very sparse when wavelet bases are used as expansion and test bases. This property is particularly attractive when dealing with integral equations [1,6-10]. Compactly supported wavelets were used as bases to transform matrix operator equations resulting from discretization of integral equations [1] and sparse matrices were obtained in all cases. Orthogonal wavelets on [0,1] for analysis of thin wire antennas and scatterers have been presented [9]. In [10] authors applied biorthogonal spline wavelets on [0,1] to the solution of integral equations in EM scattering. A biorthogonal wavelet based method of moments (BWMoM) was proposed, and numerical examples have shown that sparse matrices can generally be expected when using this method in solving integral equations defined on smooth or piecewise smooth curves. This paper provides numerical evidence on the particular advantages of using wavelet based MoM for solving large scale problems. The rest of the paper is organized as follows: In section II we outline the major issues in using biorthogonal wavelet based moment methods for solving integral equations. This includes a brief description of the biorthogonal spline wavelet bases on the interval [0,1] used in this work, followed by discussion of the discretization of the integral equations under wavelet bases. The emphasis is on the analysis of the decay behavior of the matrix coefficients. Section III provides numerical examples. 2D electromagnetic scattering is analyzed by solving the corresponding EFIE, and five cases corresponding to five different scatterer sizes were tested by using the method presented in [10]. A brief conclusion is given in section IV.

II. BIORTHOGONAL WAVELET-BASED MOM FOR THE SOLUTION OF 2D EFIE

A. Biorthogonal Spline Wavelet Bases on [0,1]

Biorthogonal spline wavelets on [0,1] at a single resolution level are composed of a finite number of so-called boundary wavelets and a finite number of interior wavelets [3,10].

Manuscript received June 3, 1998.
Q. Zhang, e-mail: zqinke@uakron.edu. N. Ida, Tel: 330-972-6525, Fax: 330-972-6487, e-mail: ida@uakron.edu.

A lowest resolution level J_0 needs to be prescribed for a specific biorthogonal wavelet pair for analysis to be realistic. The primal wavelet and dual wavelet bases are expressed as

$$\Psi = \bigcup_{j=J_0-1}^{\infty} \Psi_j , \quad \widetilde{\Psi} = \bigcup_{j=J_0-1}^{\infty} \widetilde{\Psi}_j \tag{1}$$

where Ψ_j and $\widetilde{\Psi}_j$ are the sub-bases of the primal and dual wavelets at resolution level j, respectively, and are given by

$$\Psi_j = \left\{ \psi_{j,k} \, ; \, k \in \nabla_j \right\}, \qquad \widetilde{\Psi}_j = \left\{ \widetilde{\psi}_{j,k} \, ; \, k \in \widetilde{\nabla}_J \right\} \tag{2}$$

where ∇_j and $\widetilde{\nabla}_J$ denote the shift index sets of the wavelets on [0,1] at the resolution level j for the primal and dual sides, respectively. Note that

$$\Psi_j = \Phi_{J_0} = \left\{ \psi_{J_0,k} \, ; \, k \in \Delta_{J_0} \right\}, \quad j=J_0-1 \tag{3}$$

$$\widetilde{\Psi}_j = \widetilde{\Phi}_{J_0} = \left\{ \widetilde{\psi}_{J_0,k} \, ; \, k \in \widetilde{\Delta}_{J_0} \right\}, \quad j=J_0-1 \tag{4}$$

where Φ_j and $\widetilde{\Phi}_j$ account for the sub-bases of the primal and dual scaling functions on [0,1] at the lowest resolution level J_0, and Δ_j and $\widetilde{\Delta}_j$ correspond to the shift index sets for the primal and dual scaling functions, respectively. From a single cardinal B-spline function of order d, a family of biorthogonal wavelet bases with exactness order of $\tilde{d}$ for dual scaling functions, satisfying $\tilde{d} \geq d$ and $\tilde{d}+d$=even, can be constructed [2,3]. The major features of the biorthogonal spline wavelet bases described above can be outlined as follows [3,10]:

(i). There are fixed number of left and right boundary wavelets on both the primal and dual sides for a fixed pair of $(\tilde{d}+d)$, and the number of the total wavelet functions over [0,1] at a given resolution level j is fixed, i.e., 2^j.

(ii). The sub-basis Φ_j in (3) is exact of order d on [0,1]; Similarly the sub-basis $\widetilde{\Phi}_j$ in (4) is exact of order $\tilde{d}$.

(iii). Biorthogonality relations:

$$\left(\Psi_j \, , \, \widetilde{\Psi}_{j'} \right)_{[0,1]} = \delta_{j,j'} I^{2^j} \qquad j,j' \geq J_0 - 1 \tag{5}$$

where $\left(\Psi_j \, , \, \widetilde{\Psi}_{j'} \right)_{[0,1]}$ denotes a matrix-form inner product over [0,1], I^{2^j} the unit matrix of size $2^j \times 2^j$, $\delta_{j,j}$ the delta function.

(iv). Zero-moments:

$$\int_{[0,1]} x^{\alpha} \psi_{j,k} dx = 0, \quad \int_{[0,1]} x^{\beta} \widetilde{\psi}_{j,k} dx = 0, \quad \alpha < \tilde{d}, \beta < d \, . \tag{6}$$

(v). Reisz basis property: Any function $f \in L_2(\mathbf{R}[0,1])$ has a unique expansion

$$f=\sum_{j=J_0-1}\sum_{k\in\nabla_j}\langle f,\psi_{j,k}\rangle_{[0,1]}\widetilde{\psi}_{j,k} \tag{7}$$

B. Biorthogonal Wavelet Based-MoM for the Solution of EFIE

The electric field integral equation (EFIE) for 2D EM scattering (TM case) is expressed as

$$E_z^{inc}(\mathbf{r})=\frac{k\eta}{4}\int_C J_z(\mathbf{r}')H_0^{(2)}(k|\mathbf{r}-\mathbf{r}'|)dl' \tag{8}$$

where C denotes the contour representing the surface of the scatterer. If C is smooth or piecewise smooth, then, by applying the domain decomposition and local transformation scheme described in [11], the biorthogonal wavelet bases on [0,1] described above can be lifted, thus we have the corresponding wavelet bases on the contour C. By using the dual wavelets as the trial basis, we can expand the unknown surface current in (8) as

$$J_z(\mathbf{r}')=\sum_{j=J_0-1}^{J_h}\sum_{k\in\nabla_j}J_{j,k}\widetilde{\psi}_{j,k}(\tau^{-1}(\mathbf{r}')), \tag{9}$$

where $\mathbf{r}'=\tau(\xi')$ is the compressed form of the specific two-step mapping used from the physical domain C to the domain [0,1], J_h is the pre-specified highest resolution level in the analysis. The MoM with the primal wavelets as the test basis gives the following matrix equation

$$\left(\mathbf{A}_{\widetilde{\psi},\psi}^{J_0:J_h}\right)\mathbf{J}=\mathbf{U} \tag{10}$$

The elements of the coefficient matrix $\mathbf{A}_{\widetilde{\psi},\psi}^{J_0:J_h}$ and the right hand-side vector $\mathbf{U}$ are given by

$$\left(\mathbf{A}_{\widetilde{\psi},\psi}^{J_0:J_h}\right)_{j',k',j,k}=\frac{k\eta}{4}\int_{\Omega_{j,k}}\psi_{j,k}(\xi)\varsigma(\xi)d\xi \left[\int_{\widetilde{\Omega}_{j',k'}}\widetilde{\psi}_{j',k'}(\xi')H_0^{(2)}\left(k|\mathbf{r}(\xi)-\mathbf{r}'(\xi')|\right)\varsigma(\xi')d\xi'\right] \tag{11}$$

$$(\mathbf{U})_{j,k}=\int_{\Omega_{j,k}}\psi_{j,k}(\xi)E_z^{inc}\left(\mathbf{r}(\xi)\right)\varsigma(\xi)d\xi \tag{12}$$

where $\Omega_{j,k}$ and $\widetilde{\Omega}_{j',k'}$ are the supports of $\psi_{j,k}$ and $\widetilde{\psi}_{j,k}$ respectively, $\varsigma(\xi)$ is the integral scale determined by the specific two-step mapping used in the domain transformations, and $j,j'=J_0-1,\ldots,J_h$, $k\in\nabla_j$, $k'\in\nabla_{j'}$.

C. Decay of the Matrix Coefficients

Theoretical analysis and numerical examples have shown [1,4,8,10] that when compactly supported wavelets with certain order of zero-moments are used in solving integral equations, the coefficients of the resulting matrices exhibit fast decay away from the diagonals near the singularities, and the decay is a key to achieving "sparse" matrices. The zero-moment property of the wavelet bases plays a central role in generating this decay, while other facts, e.g., the small supports of wavelets, also make important contribution. The following analysis and arguments show that with the zero-moments and small support of the underlying wavelet bases, the decay of the coefficients will be more apparent thus, a higher compression rate can be achieved when underlying systems become larger and more levels are used in analysis.

For the EFIE in (8), the kernel is the second kind Hankel function of order zero. When the argument $k|\mathbf{r}-\mathbf{r}'|$ is sufficiently large, the principal part of the Hankel function can be written as

$$H_0^{(2)}\left(k|\mathbf{r}-\mathbf{r}'|\right)\approx\frac{B_0}{\left(k|\mathbf{r}-\mathbf{r}'|\right)^{s+2}}, \tag{13}$$

and has the following estimate

$$\left|\partial_\xi^\alpha\partial_\xi^\beta H_0^{(2)}\left(k|\mathbf{r}(\xi)-\mathbf{r}'(\xi')|\right)\right|=\frac{C_\alpha(\xi)C_\beta(\xi')}{\left(k|\mathbf{r}(\xi)-\mathbf{r}'(\xi')|\right)^{s+2+\alpha+\beta}}, \tag{14}$$

where $\xi,\xi'\in[0,1]$, $C_\alpha(\xi)$ and $C_\beta(\xi')$ are determined by the two-step mappings used. The coefficients in (11) are estimated as

$$\left|\partial_\xi^\alpha\partial_\xi^\beta H_0^{(2)}\left(k|\mathbf{r}(\xi)-\mathbf{r}'(\xi')|\right)\right|=\frac{C_{d,\tilde{d}}2^{-((1+d)j'+(1+\tilde{d})j)}}{\left(dist(\Omega_{j,k},\Omega_{j',k'})\right)^{s+2+d+\tilde{d}}}, \tag{15}$$

where $dist(\Omega_{j,k},\Omega_{j',k'})$ denotes the distance from the support of the wavelet $\widetilde{\psi}_{j',k'}$ to the support of the wavelet $\psi_{j,k}$. Eq. (15) indicates that the decay rate of the coefficients is directly related to the order of the zero-moments and the sizes of the supports (and distance) of the wavelets. Higher order of the zero-moments (larger values for d and $\tilde{d}$) means faster decay; The smaller support means that more elements are off singularities, thus exhibiting decay. Another important observation is that when treating large scale problems, and more level wavelets are being used, more coefficients will have very small values compared with a smaller system, because in this case the supports of the wavelets at higher levels get smaller and smaller, and more coefficients are calculated with larger values for the term $dist(\Omega_{j,k},\Omega_{j',k'})$ in (15) due to corresponding wavelets, $\widetilde{\psi}_{j',k'}$ and $\psi_{j,k}$ being far away from each other. Because of this the matrix can be made "sparse". By this, we mean that a large number of the coefficients are very small compared with the other coefficients. Setting these small coefficients to zero has little effect on the final solutions of the matrix equation.

III. NUMERICAL EXAMPLES

A. Descriptions of the Problems

The example is a 2D EM scattering from an object which has an open structure shown in Fig. 1. The inner angle of the structure was chosen to be 90° and a TM plane wave traveling in the x-direction was assumed in the analysis.

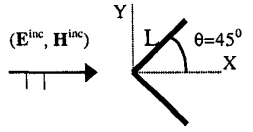

Fig. 1 An open structure illuminated by a plane wave.

The 2D electromagnetic scattering problem can be reduced to solving the same integral equation as in (8) except for the domain. The example is intended to investigate the numerical behavior of the wavelet bases for large scale problems. In computational electromagnetics the size of an underlying problem is determined by the electric size of the physical domain, measured by the wavelength λ of the electromagnetic wave. For this example if the geometric size of the object expressed in terms of the wavelength as $L=m\lambda$, then a large size means a large value of m.

In numerical analysis treating a large size problem means that a large system corresponding to a large number of the unknowns has to be solved. For example, in finite element analysis when the size of the underlying problem is large, a sufficiently fine mesh with sufficient number of nodes has to be generated. This requires solution of a large system of discretized matrix equations.

The size of the physical domain, the open structure in this example, was properly determined in the analysis. Specifically, $L=4\lambda$ was chosen for the analysis at a single level with the prescribed lowest resolution level $J_0=5$, and the higher resolution level J_h also equal to 5, i.e., $J_h=5$, because the numerical tests performed in the analysis have shown that when the structure is of this size and the lowest resolution level is chosen as $J_0=5$, one level analysis is sufficient for a given accuracy requirement.

Doubling the size of the object to $L=8\lambda$, we need doubly refined basis functions in order to achieve about the same accuracy. In finite element based methods, this can be done by doubling subdivision of the physical domain. In wavelet analysis one needs to update the basis functions to the next higher resolution level, i.e., $J_h=6$ has to be used in the expansion (9). Similarly, for the size $L=16\lambda$, the higher resolution level of $J_h=7$ is needed.

Five cases were tested in the analysis. They correspond to the scatterer sizes of $L=4\lambda$, 8λ, 16λ, 32λ and 64λ while the highest resolution levels used for these cases are $J_h=5$, 6, 7, 8, and 9, respectively, with the fixed lowest resolution level $J_0=5$. Thus, the case $L=4\lambda$ with $J_h=5$ corresponds to a single-level analysis, $L=8\lambda$ with $J_h=6$, to a 2-level analysis, etc.

In each case, the resulting matrix equation was solved with both the original dense matrix and sparse matrices by applying thresholds. If the solution from the dense matrices is called the "true" solution, the solutions from the corresponding sparse matrices are called the approximate solutions, then the approximate solutions can be evaluated by determining a proper criterion based on the "true" solution.

B *Criteria for Evaluation of the Solution Error from Sparse Matrices*

Let $J_{s;J_0:J_h}$ denote the "true" solution by using the original dense matrices, $J^{(\delta)}_{s;J_0:J_h}$ the approximate solution by applying the sparse matrices for a given threshold δ and given multilevel analysis (J_0: J_h), i.e.,

$$J_{s;J_0:J_h} = \sum_{j=J_0-1}^{J_h} \sum_{k\in\nabla_j} J_{j,k}\widetilde{\psi}_{j,k} \quad , \tag{16}$$

$$J^{(\delta)}_{s;J_0:J_h} = \sum_{j=J_0-1}^{J_h} \sum_{k\in\nabla_j} J^{(\delta)}_{j,k}\widetilde{\psi}_{j,k} \quad , \tag{17}$$

The difference between the two solutions, denoted by $\Delta J^{(\delta)}_{s;J_0:J_h}$, is given by

$$\Delta J^{(\delta)}_{s;J_0:J_h} = J_{s;J_0:J_h} - J^{(\delta)}_{s;J_0:J_h} = \sum_{j=J_0-1}^{J_h} \sum_{k\in\nabla_j} \left(J_{j,k} - J^{(\delta)}_{j,k}\right)\widetilde{\psi}_{j,k} \quad . \tag{18}$$

Two criteria can be defined for the evaluation of the solution errors:

(i). Maximum Error

The maximum error can be defined as

$$\Delta J^{(\delta)}_{max} = Max\left\{\left|\frac{\left(J_{j,k} - J^{(\delta)}_{j,k}\right)}{J_{j,k}}\right| \; ; \; j=J_0-1,\ldots,J_h,\; k\in\nabla_j\right\} . \tag{19}$$

where $\left(J_{j,k} - J^{(\delta)}_{j,k}\right)$ are the coefficients in the difference (18), $J_{j,k}$ the coefficients in the "true" solution (16).

(ii). Average Error

Projecting the difference onto the primal bases

$$\left\{\psi_{j,k} \; ; \; j=J_0-1,\ldots,J_h,\; k\in\nabla_j\right\} , \tag{20}$$

the average error can be determined by

$$\left\|\Delta J^{(\delta)}_{s;J_0:J_h}\right\|_{overall} = \frac{1}{\left\|J_{s;J_0:J_h}\right\|_{\psi}} \left(\sum_{j=J_0-1}^{J_h} \sum_{k\in\nabla_j} \left(J_{j,k} - J^{(\delta)}_{j,k}\right)^2\right)^{1/2} , \tag{21}$$

where the norm is defined by

$$\|f\|_{\psi} = \left(\sum_{j=J_0-1}^{J_h} \sum_{k\in\nabla_j} \left|\langle f,\, \psi_{j,k}\rangle_{[0,1]}\right|^2\right)^{1/2} , \tag{22}$$

and $\langle .\,,\, .\rangle_{[0,1]}$ is the inner product defined over [0,1].

C. *Numerical Results*

The proposed BWMoM in [10] has been implemented by object-oriented programming, and the resulting matrix equations were solved by a solver based on preconditioned bi-conjugate gradient method. The corresponding C++ code was run on a Cray-T90.

Fig. 2 shows the magnitudes of the wavelet coefficients in the expansion (16) for the surface currents computed with the highest resolution level J_h being 7 and the scatterer sizes $L=16\lambda$. It can be seen that the wavelet coefficients at the highest resolution level are very small compared with those at the lower levels. This suggests that the wavelet coefficients at the levels higher than the chosen levels (i.e., j=5-7) would be even smaller if further updates to the higher levels were performed. This situation was retained in the other four tests, and was both the basic starting point and expectation when the idea to perform these tests was first formed.

Fig. 3 shows the sparsity pattern of the matrix for the case $L=8\lambda$ and $J_h=6$ when the threshold $\delta=0.0008$ was applied to the original dense matrix. The dark areas correspond to the nonzero entries. Fig. 4 shows the relationships between sparsity of the matrices and the corresponding scatterer sizes when predetermined average solution errors were applied. Fig. 4 indicates that the matrices become sparser when the problem becomes larger. This may be a very interesting and useful result. Fig. 5 shows the current distributions on the scatterer surface with size $L=8\lambda$. Both the 'true" and the approximate solutions are displayed.

Table 1 shows the statistical results of the operations actually taken when solving the full and sparse matrices and their relationships with the sparsity and different thresholds for some acceptable accuracy. It can be seen that the larger the problem the more computation time is saved.

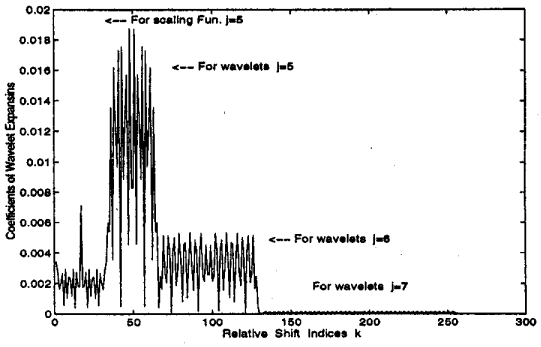

Fig. 2. Wavelet expansion coefficients for $L=16\lambda$ and $J_h=7$.

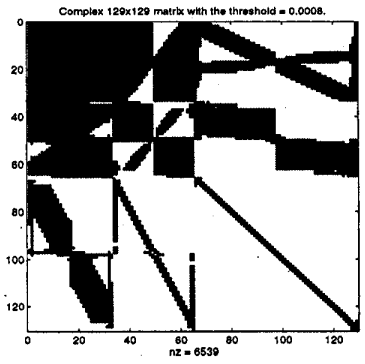

Fig. 3. Sparsity pattern for $L=8\lambda$ and $J_h=7$.

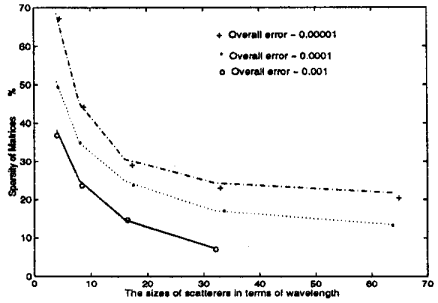

Fig. 4. Sparsity vs. the electric sizes of the object.

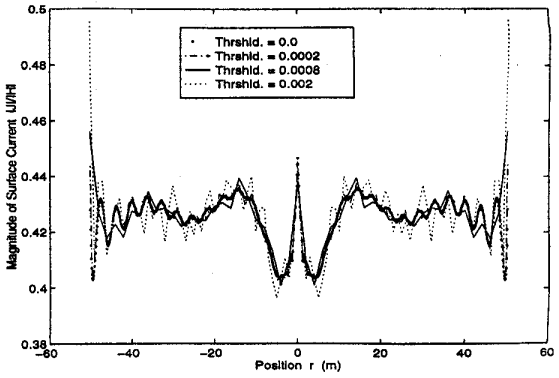

Fig. 5. Current distributions for $L=8\lambda$.

TABLE I. Execution times and sparsity versus thresholds.

Size of scatterer	4λ	8λ	16λ	32λ	64λ
Matrix N×N	65×65	129×129	257×257	513×513	1025×1025
No. of iterations	50	38	31	28	26
Thresholds	2×10^{-3}	4×10^{-4}	2×10^{-4}	5×10^{-5}	2×10^{-5}
Overall errors	$O(10^{-5})$	$O(10^{-5})$	$O(10^{-5})$	$O(10^{-6})$	$O(10^{-6})$
Sparsity α(%)	68.4	45.2	30.6	24.3	21.7
CPU (s) (full)	0.759	2.29	7.35	26.52	98.21
CPU (s) (sparse)	0.521	1.033	2.24	6.45	21.9
CPU (%) (saving)	0.314	54.9	69.5	75.6	77.7

IV. CONCLUSIONS

The wavelet-based MoM is especially suitable for analysis of large problems in the sense that the sparseness of the resulting matrices becomes more apparent as the electrical size of underlying objects increases.

REFERENCES

[1] A. G. Beylkin, R.R. Coifman and V. Rolhlin, "Fast wavelet transform and numerical algorithms I", *Comm. Pure and Appl. Math.*, 44, 1991, pp 141-183.

[2] A. Cohen, I. Daubechie, and J-C Feauveau, "Bi-orthogonal bases of compactly supported wavelets", *Comm. Pure and Appl. Math.* 45 (1992), 485-560.

[3] W. Dahmen, A. Kunoth, and K. Urban, "Biorthogonal spline-wavelets on the interval --- stability and moment conditions", *Preprint*, 1996.

[4] W. Dahmen, S. Prossdorf, and R. Schneider, "Multiscale methods for Pseudo-differential equations on Smooth Closed Manifolds", In C.K. Chui, "Wavelets: Theory, Algorithms, and Applications", 385-424, 1994.

[5] I. Daubechies, "Ten lectures on Wavelets", SIAM, Philadelphia, 1992.

[6] J. C. Goswami, A. K. Chan and C. K. Chui, "On solving first-kind integral equations using wavelets on a bounded interval," *IEEE Trans. Antennas Propagat.*, Vol. 43, Jun. 1995, pp. 614-622.

[7] K. Sabetfakhri and L. P. B. Katehi, "Analysis of integrated millimeter-wave and submillimeter-wave waveguides using orthonormal wavelet expansions", *IEEE Trans. Microwave Theory and Tech.*, Vol. 42, Dec. 1994, pp2412-2422.

[8] G. Wang, "A hybrid wavelet expansion and boundary element analysis of electromagnetic scattering from conducting objects," *IEEE Trans. Antennas Propagat.*, Vol. 43, Feb. 1995, pp. 170-178.

[9] G. Wang, "Application of wavelets on the Interval to the analysis of thin-wire antennas and scatterers," *IEEE Trans. Antennas Propagat.*, Vol. 45, May 1997, pp. 885-893.

[10] Q. Zhang and N. Ida, "Application of Biorthogonal wavelets on the interval [0,1] to 2D EM Scattering", *IEEE Trans. Mag.* Vol. 34, No. 5, Sept. 1998, pp.2728-2731.

[11] Q. Zhang, "Biorthogonal wavelet-based method of moments for EM Scattering", *PhD Dissertation*, The University of Akron, 1998.